Slug Length Estimation for Gas-liquid Slug Flow in T-shaped Microdevices with Liquid Film

Keisuke Miyabayashi, Osamu Tonomura*, Ken-ichiro Sotowa, Shinji Hasebe.

Department of Chemical Engineering, Kyoto University, Nishikyo, Kyoto 615-8510, Japan
**e-mail: tonomura@cheme.kyoto-u.ac.jp*

Abstract: To realize stable long-term operation of microdevices with gas-liquid slug flow, the slug lengths have to be monitored and controlled, because they influence mass transfer performance. In this study, an experimental investigation was carried out to analyze the gas-liquid slug flow in a T-shaped microdevice with a liquid film. The experimental result showed that the pressures in gas and liquid feeding tubes oscillate periodically along the formation of a pair of gas and liquid slugs. Then, the correlation equation between the liquid film thickness and the number of capillaries was identified on the basis of the experimental data. Based on these results, a method for estimating slug lengths and liquid film thickness from measurements of feed pressure and feed flowrate was developed. The developed method is non-invasive and does not affect slug formation or the manner of gas-liquid slug flow. Its effectiveness was assessed through an experimental case study, and the relative root mean square errors of estimated slug lengths were within 8.5%. The result show that the developed method can be applied to the monitoring of slug lengths.

Keywords: Microdevices, Gas-liquid slug flow, Liquid film, Slug length estimation, Process monitoring.

1. INTRODUCTION

When two mutually immiscible fluids, such as gas and liquid, are simultaneously fed into a micro/millimeter-scale channel, various flow patterns such as annular, dispersed and slug flows are generated as to the design and operating conditions (Shao et al., 2009). Among these, slug flow, also called Taylor flow or segmented flow, is especially attractive in a broad range of applications, such as in chemical, bio-chemical and material synthesis, drug discovery, medical diagnostics and treatments (Suryawanshi et al., 2018), due to its small residence time distribution and large interface area per fluid volume (Kreutzer et al., 2008). In addition, rapid mass transfer between two phases is achieved because the liquid interface is constantly renewed by the circulation flow inside the liquid slug (Kashid et al., 2005). As the application examples of micro/millimeter-scale channels with gas-liquid slug flow, Yasukawa et al. (2011) reported that a space-time yield of the oxidation of ethyl lactate for producing ethyl pyruvate in microdevices was ten-times larger than that in conventional devices. Takebayashi et al. (2012) reported that the direct carbonylation of nitrobenzene to phenylisocynate was conducted by using T-shaped microdevices with gas-liquid slug flow, and the isocyanate yield in microdevices was three to six times higher than that in the batch reactors. To utilize these processes in production, it is necessary to develop design and operation methods of a system that can generate slug flows with desired slug lengths, because the slug length is one of the important state variables that affect mass transfer between two different phases (Aoki et al., 2011).

In the operation of the slug flow systems, a process monitoring method is important for realizing stable long-term operation of microdevices, because abnormal conditions such as the deposition of solid on the surface of channels are likely to occur. Such disturbances affect the physical condition of the channels and change the slug lengths to undesired values. Thus, for a long period operation, process monitoring systems that can detect such unacceptable condition are necessary. Optical methods (Nguyen et al., 2006, Ide et al., 2009) and electrical methods (Ye et al., 2011) have been proposed as the measuring methods of void fraction in micro/millimeter-scale channels. Though these methods are applicable to the monitoring of slug lengths, there are some drawbacks. As the optical method requires the placement of the windows on the channels to visualize the slug flow, it is not applicable to microdevices made of opaque materials. The electrical method uses the electrical resistance and capacitance of fluid in the micro/millimeter-scale channels to estimate the condition in the channel. If the device is made of electrically-conductive materials such as stainless steel, complicated electrically-insulated placement of electrodes is required. Hence, the objective of this research is to develop alternatives to the conventional measuring methods of slug lengths in micro/millimeter-scale channels.

In our previous work (Miyabayashi et al., 2015), an estimation method of slug lengths from the measurements of feed pressure of gas or liquid was developed for T-shaped micro/millimeter-scale channels. By this method, the slug lengths can be monitored without complicated processing, such as the placement of the windows and electrodes on channels. However, the usefulness of the developed method has only been confirmed for the slug flow process in the absence of a liquid film, which may form around the gas slug depending on the design and operating conditions. When the liquid film is formed, the mass transfer between two phases is promoted due to the increase in the gas-liquid contact area (van Baten and Krishna, 2004, Yue et al., 2009, Aoki et al., 2011). The previously developed method cannot be directly applied

to the slug flow process in the presence of a liquid film, because the cross-sectional area of the slug, which changes depending on the thickness of the liquid film, is included as a variable in the model used for estimating the slug length. Therefore, the purpose of this study is to develop a method for estimating the slug length in the presence of the liquid film by incorporating the method for estimating the liquid film thickness into the previously developed slug length estimation method.

The outline of this paper is as follows: after explaining a gas-liquid slug flow experimental system composed of a T-shaped micromixer and a reaction tube in Section 2, the relationship between the flow behavior and feed pressure changes of gas and liquid is discussed through experimental observation on the gas-liquid slug flow generation in the micromixer in Section 3. In Sections 4 and 5, the slug flow in the presence of the liquid film is modeled and the model parameter is identified from the expermental data. In Section 6, a method for estimating the slug length in the presence of the liquid film is developed, and the effectiveness of the developed method is verified through case studies.

2. EXPERIMENTAL SETUP

Figure 1 shows a schematic diagram of the constructed experimental system. Nitrogen filled in a gas cylinder and liquid dodecane filled in a syringe are supplied to an acrylic T-shaped micromixer (Sanko Seiki Kogyo Co., Ltd.) at constant flow rates, Q_G and Q_L [m^3/s], by using a mass flow controller (FCST-1005LC, Fujikin) and a syringe pump (PHD-2000, Harvard), respectively. Similar experiments on gas-liquid slug flow with nitrogen-dodecane have already been reported (Molla et al., 2011). A high-speed microscope (VW-6000, Keyence) is used to observe the formation of gas-liquid slug flow in the T-shaped micromixer. Pressure sensors (PA-830-101G-10, Nidec Copal Electronics) are installed in the gas and liquid feeding tubes to acquire pressure data. In addition, a polytetrafluoroethylene (PTFE) tube (GL Science) is connected to the mixer outlet as a reaction tube. Two digital fiber-optic sensor units (FU-L51Z, Keyence) are installed in the reaction tube side by side in the flow direction at a point 10 cm from the outlet of the mixer. When gas and liquid flow at that point, the light transmittance in the cross-sectional direction of the tube changes, which is acquired as a voltage signal. The outlet of the reaction tube is immersed in a beaker filled with dodecane that is open to the atmosphere. Table 1 shows the materials, inner diameters and lengths of (i) gas and liquid feeding tubes, (ii) T-shaped micromixer, and (iii) reaction tube. All tubes and mixer that make up this experimental system have a circular cross-sectional shape.

Table 1. Size and material of tubes and T-shaped micromixer.

		I.D. (mm)	Length (mm)	Material
(i)	Feeding tube	1.00	100	FEP
(ii)	Micromixer	1.30	40 for all branches	PMMA
(iii)	Reaction tube	0.50	200	PTFE

(Note) FEP: fluorinated ethylene propylene, PMMA: polymethyl methacrylate, PTFE: polytetrafluoroethylene, I.D.: inner diameter.

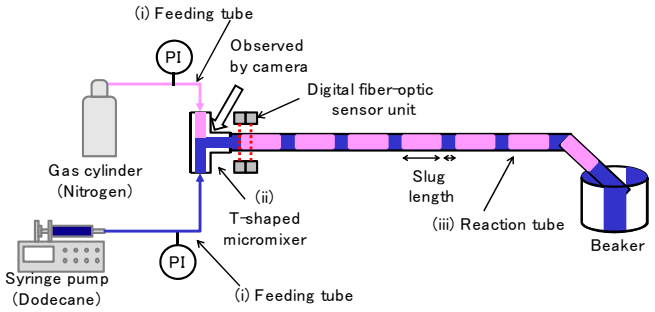

Figure 1. Gas-liquid slug flow experimental system.

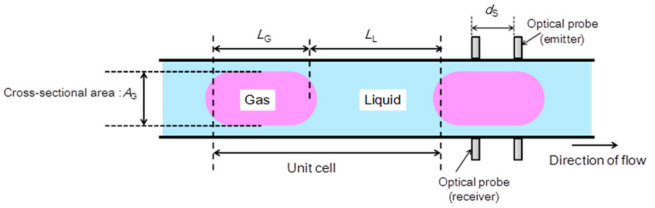

Figure 2. Slug flow in the reaction tube with digital fiber-optic sensor units.

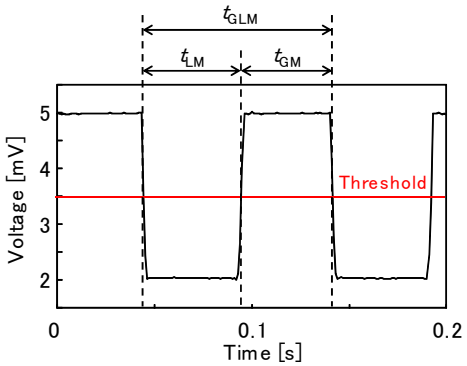

Figure 3 Voltage data obtained by a digital fiber-optic sensor unit.

A digital fiber-optic sensor unit, which consists of a pair of an emitter and a receiver, and data processing method are explained below. As shown in Fig. 2, two sets of digital fiber-optic sensor units are installed with a certain interval d_S [m], which is set to 4 mm in this experiment. The light transmittance corresponding to gas and liquid slugs is obtained as voltage as shown in Fig. 3. When the gas slug is detected, the light transmittance, that is, the voltage is large. In this study, the transit times of a gas slug and a liquid slug at an optical probe position are set as t_{GM} [s] and t_{LM} [s], respectively. The sum of them, that is, the transit time of a pair of gas and liquid slugs at the optical probe position, is defined as t_{GLM} [s]. In order to obtain t_{GM}, t_{LM}, and t_{GLM} from the voltage data as shown in Fig. 3, a threshold value for distinguishing between gas and liquid needs to be given. It is set to the average of the maximum voltage value and the minimum voltage value. Furthermore, the slug flow velocity u_{GL} [m/s], gas slug length L_G [m], and liquid slug length L_L [m] can be calculated from

the following equations, on the basis of the time Δt_S [s] at which the slug passes between two sensor units.

$$u_{GL} = \frac{d_S}{\Delta t_S} \quad (1)$$

$$L_G = u_{GL} t_{GM} \quad (2)$$

$$L_L = u_{GL} t_{LM} \quad (3)$$

All experiments in this study are performed at room temperature (298 K) and atmospheric pressure (101.3 kPa). Since the heat transfer performance of the microdevices is high and the temperature field inside them can be regarded as uniform, the temperature dependence of the fluid physical properties can be negligible. On the other hand, it should be noted that the pressure in the reaction tube at the installation position of the sensor units is higher than the atmospheric pressure due to the pressure loss of the slug flow through the tube, which may affect Q_G and L_G. Therefore, in this study, when expressing Q_G and L_G under the standard state (273 K, 101.3 kPa), they are described as Q_{GS} [m^3/s] and L_{GS} [m], respectively, which are converted on the basis on the gas state equation.

3. RELATIONSHIP BETWEEN SLUG FLOW GENERATION AND FEED PRESSURE FLUCTUATION

Using the experimental system shown in Fig. 1, the gas-liquid slug flow generation in the mixer was observed by the microscope and the gas and liquid feed pressures were measured at the same time. Figure 4 shows the gas and liquid feed pressure measurements obtained under $Q_{GS} = Q_L = 1.0$ mL/min. To make it easier to understand the pressure change, the smoothing line obtained by the Savitzky-Golay filter (Savitzky and Golay, 1964) is also shown by the black line. Figure 5 shows the formation behavior of gas and liquid slugs in the mixer under $Q_{GS} = Q_L = 1.0$ mL/min. Each photograph in Fig. 5 was taken at each time from A to E in Fig. 4. It can be seen from Fig. 5 that gas and liquid alternately flow out from the mixer to the subsequent reaction tube. Figures 4 and 5 show that the gas and liquid feed pressures change

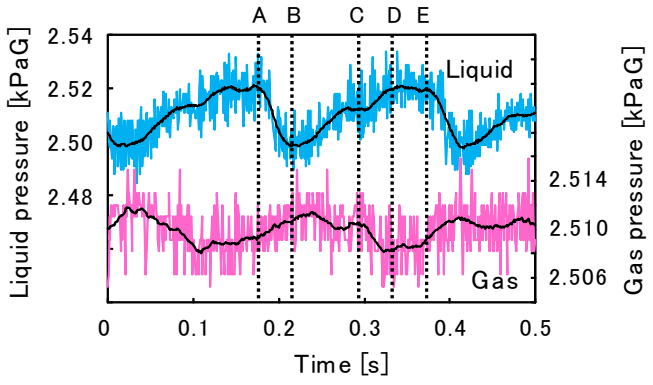

Figure 4. Profiles of gas and liquid pressure changes: $Q_G = Q_L = 1.0$ mL/min.

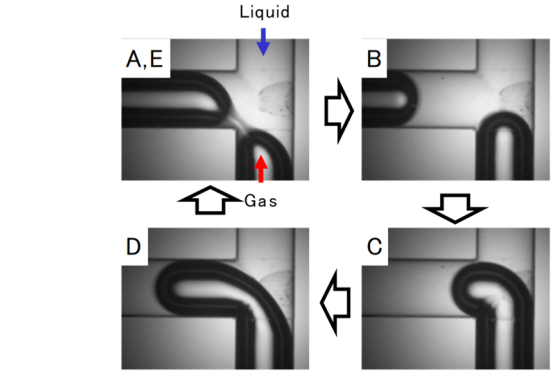

Figure 5. Photos of flow behavior in T- mixer. (A, E) Liquid blocks gas flow and starts flowing to the succeeding tube, (B) Liquid flows to the succeeding tube, and gas is penetrating to the confluence part, (C) Gas blocks liquid flow and starts flowing to the succeeding tube, and (D) Gas flows to the succeeding tube, and liquid is penetrating to the confluence part.

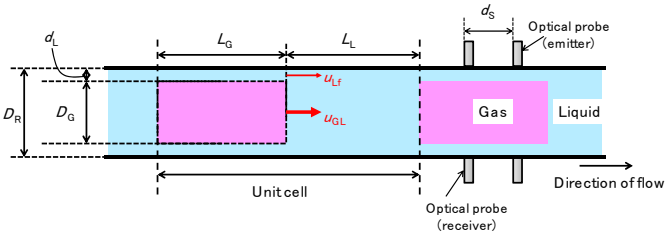

Figure 6. Model of gas-liquid slug flow with wall film.

periodically in a wavy manner and that a pair of gas and liquid slugs are generated during one cycle, corresponding from A to E, of this pressure fluctuation. In the following sections, liquid pressure data is used, where pressure changes are relatively easy to understand.

4. MODEL OF SLUG FLOW IN THE PRESENCE OF A LIQUID FILM

In the constructed experimental system, it is considered that a liquid film is formed around the gas slugs as shown in Fig. 2, because the reaction tube made of a hydrophobic material has high wettability to dodecane. In this study, the slug flow in the presence of the liquid film is modeled as shown in Fig. 6. It is assumed that the liquid film has a uniform thickness d_L [m] and flows in the axial direction at an average flow velocity u_{Lf} [m/s]. The gas slug surrounded by the liquid film is regarded as a cylinder with a diameter of D_G [m] and flows at a flow velocity of u_{GL} [m/s]. Based on this model, the thickness and flow velocity of the liquid film are estimated from experimental results in the next section.

5. THICKNESS AND FLOW VELOCITY OF LIQUID FILM

The thickness and flow velocity of the liquid film are experimentally evaluated. Subsequently, the introduction of a

previously proposed model for estimating the liquid film thickness into this study is considered.

5.1 Experimental evaluation

According to the model shown in the previous section, the d_L and u_{Lf} of the liquid film is derived from the measured values obtained by the digital fiber-optic sensor units and the feed flow rates of the mass flow controller and syringe pump, by using Eqs. (1)-(3) and the following equations:

$$Q_G = u_{GL} A_G \frac{L_G}{L_G + L_L} \tag{4}$$

$$Q_G + Q_L = u_{GL} A_G + u_{Lf}(A_R - A_G) \tag{5}$$

$$d_L = \frac{A_R^{1/2} - A_G^{1/2}}{\pi} \tag{6}$$

$$A_G = \pi\left(\frac{D_G}{2}\right)^2 \tag{7}$$

$$A_R = \pi\left(\frac{D_R}{2}\right)^2 \tag{8}$$

Here, A_G [m^2] is the cross-sectional area of the gas slug having diameter D_G, D_R [m] is the inner diameter of the reaction tube, and A_R [m^2] is the cross-sectional area of the reaction tube. The set values of the mass flow controller and the syringe pump are assigned to Q_G and Q_L, respectively. D_R is 0.5 mm in the experimental system of this study. A_G is calculated using Eqs. (1)-(4). Then, using the calculated A_G and Eqs. (5)-(8), u_{Lf} and d_L are derived. Table 2 shows the d_L and u_{Lf} derived for various feed flowrates. Since the value of u_{Lf} is very small, the u_{Lf} in Eq. (5) is set to 0 for further examination of this study.

Table 2. Experimental results for u_{GL}, d_L, u_{Lf} and Ca.

(Q_{GS}, Q_L) [mL/min]	u_{GL} [m/s]	d_L [μm]	u_{Lf} [×10^{-15} m]	Ca [×10^{-3}]
(1.0, 0.5)	0.144	9.44	0.00	4.99
(1.0, 1.5)	0.239	11.12	-0.77	8.27
(1.0, 2.0)	0.283	9.78	-0.44	9.77
(1.0, 2.5)	0.334	11.80	-1.46	11.55
(1.0, 3.0)	0.376	10.31	0.00	13.00
(1.0, 4.0)	0.479	12.97	0.00	16.56
(1.0, 5.0)	0.599	18.11	0.48	20.71
(2.0, 2.0)	0.386	11.40	0.00	13.36
(2.0, 3.0)	0.497	15.58	-0.56	17.17
(2.0, 4.0)	0.605	17.89	-0.98	20.92
(2.0, 5.0)	0.708	18.57	-0.47	24.47

5.2 Estimation model for liquid film thickness

In the previous section, it was shown that the flow velocity of the liquid film was negligibly small. In Section 3, it was shown that a pair of gas and liquid slugs was generated during one cycle of pressure fluctuation. In this section, the lengths of gas and liquid slugs in the reaction tube are estimated from the pressure fluctuation period t_{GL} [s] obtained through the feed pressure measurement, by using the following equations:

$$L_G^* = Q_G t_{GL} / A_G \tag{9}$$

$$L_L^* = Q_L t_{GL} / A_G \tag{10}$$

where L_G^* and L_L^* are estimates of L_G and L_L. If A_G is determined, the lengths of the gas and liquid slugs in the reaction tube can be estimated.

In the previous section, the liquid film thickness was estimated from u_{GL}, L_G, L_L measured by the digital fiber-optic sensor units, and as a result, A_G was determined from the estimated liquid film thickness. However, the digital fiber-optic sensor units are not always available in the actual process. In this section, the use of previously proposed models for estimating the liquid film thickness is investigated. The model by Aussillous and Quere (2000) is used in this study, which is given by the following equations:

$$\frac{2d_L}{D_R} = \frac{\alpha Ca^{\frac{2}{3}}}{1 + \beta \times \alpha Ca^{\frac{2}{3}}} \tag{11}$$

$$Ca = \frac{\mu_L u_{GL}}{\sigma_L} \tag{12}$$

where Ca [-] is the number of capillaries based on the liquid side, μ_L [Pa·s] is the liquid viscosity, σ [N/m] is the surface tension of the liquid, and α [-] and β [-] are the fitting parameters. Under the condition of Ca < 1.4, the effectiveness of α and β identified from the experimental results was confirmed (Aussillous and Quere, 2000). Eq.(11) can be transformed as follows:

$$\left(\frac{2d_L}{D_R}\right)^{-1} = \frac{1}{\alpha} Ca^{-\frac{2}{3}} + \beta \tag{13}$$

All the experimental results shown in Table 2 were plotted on

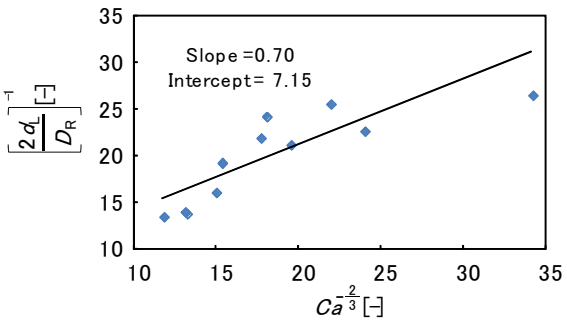

Figure 7. Relationship between $Ca^{-\frac{2}{3}}$ and $\left(2d_L/D_R\right)^{-1}$.

Table 3. Estimation results of d_L, L_G, and L_L.

(Q_{GS}, Q_L) [mL/min]	t_{GL} [s]	d_L^* / d_L [μm]	L_{GS}^* / L_{GS} [cm]	L_L^* / L_L [cm]
(1.0, 0.5)	0.258	8.03 / 9.44	2.26 / 2.36	1.13 / 1.18
(1.0, 1.0)	0.201	9.18 / 8.14	1.77 / 1.82	1.77 / 1.82
(1.0, 1.5)	0.286	10.30 / 11.12	2.53 / 2.65	3.79 / 3.98
(1.0, 2.0)	0.172	11.13 / 9.79	1.53 / 1.59	3.06 / 3.17
(1.0, 2.5)	0.250	11.99 / 11.80	2.23 / 2.34	5.58 / 5.85
(1.0, 3.0)	0.234	12.62/ 10.31	2.09 / 2.16	6.28 / 6.49
(1.0, 4.0)	0.219	13.95 / 12.97	1.97 / 2.07	7.86 / 8.26
(1.0, 5.0)	0.198	15.22 / 18.11	1.79 / 1.95	8.93 / 9.76
(2.0, 2.0)	0.212	12.77 / 11.40	3.78 / 3.94	3.78 / 3.94
(2.0, 3.0)	0.163	14.15 / 15.58	2.94 / 3.15	4.41 / 4.73
(2.0, 4.0)	0.127	15.28 / 17.89	2.30 / 2.51	4.60 / 5.01
(2.0, 5.0)	0.108	16.18 / 18.57	1.96 / 2.14	4.90 / 5.36

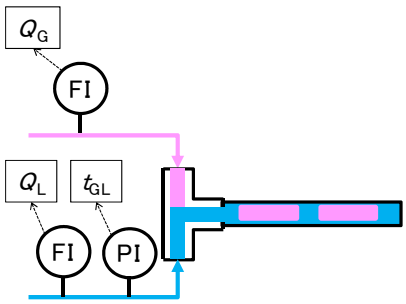

Figure 8. Configuration example of sensors installed to a T-shaped microdevice.

the plane where $Ca^{-\frac{2}{3}}$ is the horizontal axis and $\left(2d_L/D_R\right)^{-1}$ is the vertical axis, using the physical properties of μ_L = 0.00136 Pa·s and σ_L = 0.0393 N/m. Then, α and β can be derived from the slope and intercept of the approximate straight line obtained by the least squares method, as shown in Fig. 7. As a result, α and β were determined to be 1.43 and 7.15, respectively.

6. SLUG LENGTH ESTIMATION

In this section, the gas and liquid slug lengths and the liquid film thickness are estimated from the measurements of the feed pressure and the gas and liquid feed flowrates. Here is how to get those estimates: The slug flow velocity u_{GL} can be expressed by

$$u_{GL} = \frac{Q_G + Q_L}{A_G} = \frac{Q_G + Q_L}{\pi\left(\frac{D_R}{2} - d_L\right)^2} \tag{14}$$

Substituting this equation into Eq.(12), Ca is regarded as a d_L-only function, and given Q_G and Q_L, d_L is calculated from Eqs.(11) and (12). Then, the calculated d_L is used to derive A_G from Eq.(6), and the derived A_G is used to obtain u_{GL} from Eq.(14). Furthermore, t_{GL} given by the pressure sensor is used to estimate L_G and L_L from Eqs.(9) and (10), respectively.

The estimation results are shown in Table 3. The superscript * represents the estimated values, and the values of the variables without * were obtained using the digital fiber-optic sensor units. Each value is the average value for one minute. The result of (Q_{GS}, Q_L) = (1.0, 1.0) is the result under the condition not used for the estimation of the coefficients α and β. It was shown that the gas and liquid slug lengths can be estimated with a relative error of up to 8.5% of the measured values under every flow rate condition.

7. CONCLUSIONS

In this study, a gas and liquid slug length estimation method based on gas or liquid feed pressure measurement was investigated under the condition that a liquid film is formed on the inner wall surface of the micro/millimeter-scale channels. In the experiment, a gas-liquid slug flow generation system was constructed in which dodecane and nitrogen were supplied as liquid and gas, respectively, into a Teflon tube used as the reaction tube. Through the measurement of gas and liquid feed pressures and the observation of flow behavior in the T-shaped mixer, it was clarified that the gas and liquid feed pressures oscillate according to the slug flow generation and that one cycle of the oscillation is equal to the time it takes for a pair of gas and liquid slugs to be produced. After that, the liquid film thickness was examined on the basis of the mass balance of the gas-liquid slug flow in the reaction tube, using the slug flow velocity obtained by the digital fiber-optic sensor units and the gas and liquid feed flow rates. In addition, the parameters in the correlation equation between the liquid film thickness and the number of capillaries were determined from the experimental data. Based on these results, a method for estimating the liquid film thickness and the slug lengths was proposed from the gas or liquid feed pressure measurement, the gas and liquid feed flow rates, and the gas and liquid physical properties. It was confirmed that the slug lengths can be accurately estimated within 8.5% of the measured value by using the developed estimation method. Finally, Fig. 8 shows a configuration example of sensors required when the method proposed in this study is applied to a T-shaped microdevice. The gas and liquid feed flowrates are acquired by the flow sensors (FIs) installed in the gas and liquid feeding channels, and the gas-liquid slug generation cycle is acquired by the pressure sensor (PI) installed in the liquid feeding channels. Based on these acquired data, it is possible to estimate the the gas and liquid slug lengths in addition to liquid film thickness, provided that the parameters in Eq.(11) are determined. In this study, a monitoring method of slug length in a single channel microdevice was discussed. The next target is to expand the proposed method to multi-channel microdevices with slug flow.

ACKNOWLEDGEMENT

This work was partially supported by the Grant-in-Aid for Scientific Research (C) (No. 19K05140) and a project, Development of Continuous Production and Process Technologies of Fine Chemicals, commissioned by the New Energy and Industrial Technology Development Organization (NEDO).

REFERENCES

Aoki, N., Tanigawa, S., and Mae, K. (2011) Design and operation of gas-liquid slug flow in miniaturized channels for rapid mass transfer, *Chem. Eng. Sci.*, 66 6536-6543.

Aussillous, P. and Quere, D. (2000) Quick deposition of a fluid on the wall of a tube, *Physics of Fluids*, 12(10) 2367-2371.

Ide, H., Kimura, R., and Kawaji, M. (2009) Optical measurement of void fraction and bubble size distributions in a microchannel, *Heat Transfer Eng.*, 28, 713-719.

Kashid, M.N., Gerlach, I., Goetz, S., Franzke, J., Acker, J.F., Platte, F., Agar, D.W., and Turek, S. (2005) Internal circulation within the liquid slugs of a liquid–liquid slug-flows capillary microreactor, *Ind. Eng. Chem. Res.*, 44, 5003-5010.

Kreutzer, M.T., Gunther, A., and Jensen, K.F. (2008) Sample dispersion for segmented flow in microchannels with rectangular cross section, *Anal. Chem.*, 80(5) 1558-1567.

Miyabayashi, K., Tonomura, O., and Hasebe, S. (2015) Estimation of gas and liquid slug lengths for T-shaped microreactors, *Chem. Eng. J.*, 262, 1137-1143.

Molla, S., Eskina E., and Mostowfi, F. (2011) Pressure drop of slug flow in microchannels with increasing void fraction: experiment and modeling, *Lab Chip*, 11, 1968-1978

Nguyen, N., Lassemono, S., and Chollet, F.A. (2006) Optical detection for droplet size control in microfluidic droplet-based analysis systems, *Sens. Actuators B Chem.*, 117(2), 431-436.

Savitzky, A. and Golay, M.J.E. (1964) Smoothing and differentiation of data by simplified least squares procedures, *Analyt. Chem.*, 36(8) 1627-1639.

Shao, N., Gavriilidis, A., and Angeli, P. (2009) Flow regimes for adiabatic gas-liquid flow in microchannels, *Chem. Eng. Sci.*, 64, 2749-2761.

Suryawanshi, P.L., Gumfekar, S.P., Bhanvase, B.A., Sonawane, S.H., and Pimplapure, M.S. (2018). A review on microreactors: reactor fabrication, design, and cutting-edge applications. *Chem. Eng. Sci.*, 189, 431-448.

Takebayashi, Y., Sue, K., Yoda, S., Furuya, T., and Mae, K. (2012) Direct carbonylation of
nitrobenzene to phenylisocyanate using gas–liquid slug flow in microchannel, *Chem. Eng. J.*, 180, 250-254.

van Baten, J.M. and Krishna, R. (2004) CFD simulations of mass transfer from Taylor bubbles rising in circular capillaries, *Chem. Eng. Sci.*, 59 2535-2545.

Yasukawa, T., Ninomiya, W., Ooyachi, K., Aoki, N., and Mae, K. (2011) Enhanced production of ethyl pyruvate using gas–liquid slug flow in microchannel, *Chem. Eng. J.*, 167, 527-530.

Ye, J., Peng, L., Wang, W., and Zhou, W. (2011) Optimization of helical capacitance sensor for void fraction measurement of gas-liquid two-phase flow in a small diameter tube, *IEEE Sens. J.*, 11(10) 2189-2196.

Yue, J., Luo, L., Gonthier, Y., Chen, G., and Yuan, Q. (2009) An experimental study of air-water Taylor flow and mass transfer inside square microchannel, *Chem. Eng. Sci.*, 64 3697-3708.